

Downscaling of MODIS Land Surface Temperature to LANDSAT Scale Using Multi-layer Perceptron

Choe, Yu-Jeong¹⁾ · Yom, Jae-Hong²⁾

Abstract

Land surface temperature is essential for monitoring abnormal climate phenomena such as UHI (Urban Heat Islands), and for modeling weather patterns. However, the quality of surface temperature obtained from the optical space imagery is affected by many factors such as, revisit period of the satellite, instance of capture, spatial resolution, and cloud coverage.

Landsat 8 imagery, often used to obtain surface temperatures, has a high resolution of 30 meters (100 meters rearranged to 30 meters) and a revisit frequency of 16 days. On the contrary, MODIS imagery can be acquired daily with a spatial resolution of about 1 kilometer. Many past attempts have been made using both Landsat and MODIS imagery to complement each other to produce an imagery of improved temporal and spatial resolution. This paper applied machine learning methods and performed downscaling which can obtain daily based land surface temperature imagery of 30 meters.

Keywords : Downscaling, Land Surface Temperature, Multi-layer Perceptron, Random Forest, Landsat, MODIS

1. Introduction

LST (Land Surface Temperature) is essential in many applications such as monitoring heat pattern or crop monitoring by analyzing the relation between vegetation and temperature (Park, 2001; Jee *et al.*, 2014; Kim, 2016). Landsat satellites, which include sensors to measure surface temperatures, have a revisit frequency of 16 days, but are very weather dependent and prone to cloud coverage.

On the other hand, MODIS satellite imagery, which is captured every day, have a spatial resolution of 1 kilometer, which makes it difficult to determine the temperature of dense urban region. Downscaling technique is performed in such situation to complement the problems and increase both the temporal and spatial resolution.

In meteorology, downscaling refers to the method of

increasing the spatial resolution and interpolating the pixel values by referring to other related image values. GCM (General Circulation Model) is a mathematical downscaling technique used in meteorology, which is frequently used for expressing the global range of seasonal and annual weather change. However, this technique has the limitation that it is applicable for only low spatial resolution imagery (Wilby and Wigley, 1997). To overcome this limitation of GCM, dynamical calculation and statistical calculation method of downscaling were introduced in the following years (Stathopoulou and Cartalis, 2009; Zakšek and Oštir, 2012; Bonafoni, 2016). Although dynamical downscaling method can obtain a higher spatial resolution than GCM, the computation process is complicated and requires vast amount of data, and the interpretation of the results is only possible with a high level of expertise. In contrast to dynamical

Received 2017. 08. 01, Revised 2017. 08. 23, Accepted 2017. 08. 29

1) Dept. of Geoinformation Engineering, Sejong University (E-mail: choeyujeong@sju.ac.kr)

2) Corresponding Author, Member, Dept. of Geoinformation Engineering, Sejong University (E-mail: jhyom@sejong.ac.kr)

This is an Open Access article distributed under the terms of the Creative Commons Attribution Non-Commercial License (<http://creativecommons.org/licenses/by-nc/3.0>) which permits unrestricted non-commercial use, distribution, and reproduction in any medium, provided the original work is properly cited.

downscaling, statistical downscaling is easy to interpret and to compute. However, downscaling is performed only with previous weather data, so this method is not reliable if input data is insufficient (Trzaska and Schnarr, 2014).

Attempts were also made to incorporate machine learning methods to downscaling. Most of them used single layer perceptron as the unique hidden layer (Yang *et al.*, 2010; Kolios *et al.*, 2013; Bonafoni and Tosi, 2017). These early attempts did not produce satisfactory results because these models could not generalize the phenomenon, and there was not sufficient number of neurons to grasp the close relationship between the input data and the independent variables. Other attempts in machine learning included the random forest technique, which besides being computationally simple, does not require much hardware resources, and also produced good results (Hutengs and Vohland, 2016). They performed the downscaling of 1 kilometer resolution of MODIS imagery to 240 meters using the random forest method. This resolution is insufficient for detecting abnormal climate or monitoring temperature for UHI. Likewise, downscaling has also been performed using support vector regression, another machine learning method, but the output resolution was 1 kilometer (Keramitsoglou *et al.*, 2013).

In this study, downscaling to high spatial resolution of 30 meters was performed using MLP (Multi-layer Perceptron) using multiple hidden layers. Downscaling with MLP produced results of less than 3°C at 30 meter ground resolution. This is of higher spatial resolution than reported results by GCM or random forest method, and once a model is generated, it is easier to predict and to calculate than the forementioned dynamical downscaling method. In the feature design process of the hidden layers, features were classified into temporal periods of daily data, seasonal data, and fixed data (unchanging data such as digital elevation model). Since the features were selected separately, there is an advantage that the fixed data can be used repeatedly.

2. Experiment Data and Methodology

2.1 Experiment data

For accurate prediction of LST, data acquired at different days of the season were used during the modeling process.

Five Landsat 8 cloudless images from September, 2013 to May, 2016 were selected as the label data for the machine learning computation. Other feature data of the same dates were also collected and went through the preprocessing procedure. The preprocessing procedure is a very tedious job of carefully preparing the data by clipping and resampling the images to the same size, coordinates, cell size, and data type. They must also be standardized and checked for outliers, which must be imputed.

2.1.1 Daily data

The daily data are MODIS LST images. For training, MODIS data of the same day as Landsat 8 LST images are used, and the resulting model is then used with other MODIS data for prediction. The MODIS LST images were resampled to 30 meters to match the LST image of Landsat images. Landsat LST were obtained by substituting thermal infrared bands into equations provided by the USGS (United States Geological Survey). Experiments later showed that the MODIS independent variable contributes significantly to the prediction of daily 30 meter downscaling.

2.1.2 Seasonal data

Three seasonal independent variables were added to determine the temperature of each area. First, NDVI (Normalized Difference Vegetation Index) was selected to be an independent variable that can grasp the characteristics of vegetation, park, and mountain in the study area. In addition, the NDVI has been reported to have been a major factor which determines the LST (Bhang and Lee, 2017). NDWI (Normalized Difference Water Index) also was used to estimate water in the study area, that is, river and lake values. Seasonal data is useful for efficient experimentation because a representative data can be reused without having to collect it for each day.

2.1.3 Fixed data

For paved surface which increases the urban temperature, NDBI (Normalized Difference Built-up Index) was used to determine the distribution and characteristics of buildings and artificial structure. DEM was also used as the fixed data and since the energy released according to

surface characteristics is different, it was considered as an independent variable affecting temperature. Table 1 shows the resolution and source of datasets. Daily data was obtained from NASA Earth Data, and seasonal data and NDBI of fixed data were obtained by band combination of landsat images obtained from Landsat images. DEM was acquired from the Ministry of Land, Transport and Maritime Affairs with a spatial resolution of 5 meters. Table 2 shows statistics of one sample dataset, May 19, 2016. The temperatures of MODIS and Landsat are almost similar but show a large difference at maximum temperature. This is because higher spatial representation of the temperature is possible with Landsat imagery. NDBI, NDVI, and NDWI are represented by values between -1 and 1.

Table 1. Resolutions and sources of datasets used in this study

		Spatial Resolution	Temporal Resolution	Source
Daily	MODIS	1kilometer	1 day	NASA Earth Data
	LANDSAT	30m	16 days	
Seasonal	NDVI	30m	16 days	
	NDWI			
Fixed	NDBI	30m	16 days	NASA Earth Data
	DEM	5m	Non-changing	Ministry of Land, Infrastructure and Transport

Table 2. Statistics of dataset_May 19, 2016

	MODIS [°C]	NDBI	NDVI	NDWI	DEM [m]	Landsat [°C]
Mean value	28.09	0.67	0.06	0.08	47.68	27.47
Standard Deviation	1.01	0.09	0.31	0.27	40.8	2.71
Minimum value	25.33	0.13	-1	-0.54	10	20.58
Maximum value	30.65	1.0	0.77	1.0	340	41.92

2.2 MLP design and experiment

2.2.1 MLP design

The operations of a typical ANN (Artificial Neural Network) is shown in Fig. 1. The ANN consists of an input layer, a hidden layer and an output layer, and is called a single layer perceptron when there is one hidden layer and a multi-layer perceptron when the number is two or more. The independent variables of the input layer are transformed to hidden layer values by weights in the forward propagation stage. The differences between the prediction and the true target are obtained through the loss function. In regression of machine learning, the loss function mainly uses RMSE (Root Mean Square Error). After the loss is computed, weights are updated again using the optimizer in the back propagation stage. This loops continue until the loss converged to a minimum value. The final weight values are then used to compute unknown target values with new sets of input layers (Chollet, 2017).

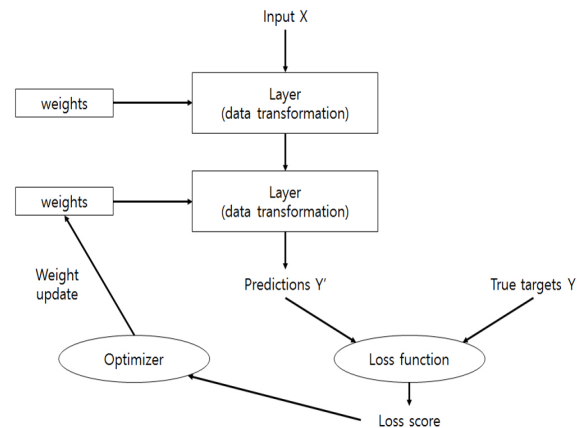


Fig. 1. Operation of artificial neural network

MLP is more efficient than conventional ANN of single layer, because with multiple layers it can extract more detailed characteristics between independent and dependent variables. The structure of MLP in this study is shown in Fig. 2. MODIS LST, NDVI, NDWI, NDBI, and DEM were used as the features in the input layer. The number of hidden layers is 4, and the number of neuron is set to 15, 10, 8, and 5 for each layer respectively. Experiments showed that the number of neurons did not significantly affect the results.

Generally, as the model gets more complex, the bias

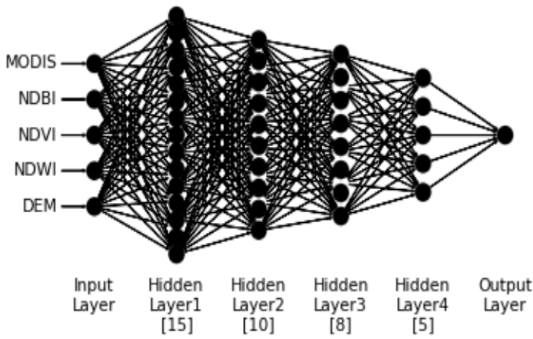


Fig. 2. Architecture of multi-layer perceptron

continues to decrease whereas the variance increases. During training phase, the accuracy will increase as the model gets more complex. But at some point, increasing the model complexity will result in the decrease of accuracy in the testing phase, because the model has been overfitted to the training data. The model design should consider selecting the optimal model complexity which will satisfy both training accuracy and testing accuracy as shown in Fig. 3 (Trevor *et al.*, 2008).

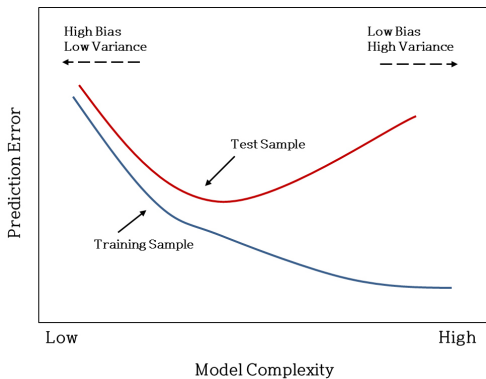


Fig. 3. Test and training error as a function of model complexity

The learning rate is selected as 0.001, which is relatively slow, but this is compensated by parallel processing using GPU. As a result of experimenting various hyper-parameters with our model, it was confirmed that the cost stabilize after about 500 epochs. The optimization function uses Adam Gradient Descent method, which is commonly used in the neural network regression problem. ReLU (Rectified Linear Unit) function was chosen as the nonlinear function to deal

with the gradient vanishing problem. MSE (Mean Square Error) was used as the cost function, as it is commonly used in regression.

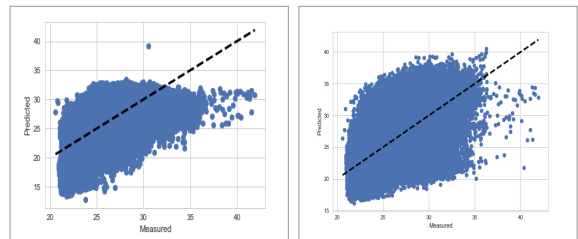
2.2.2 Validation

In order to verify the accuracy of the MLP model, 5 fold validation set was planned. One image was excluded from the 5 images, and the 4 selected images were used as the training set and the excluded image was used the test set. This was repeated to get 5 RMSE of the differences between the actual image temperature and the predicted image temperature. Also, results from random forest method was computed and is compared as shown in Table 3. Overall, MLP showed less RMSE than random forest and less standard deviation between errors. Both methods were well predicted for the September 16, 2013 sample and the October 5, 2014 sample was the worst.

Table 3. Cross validation comparison for the MLP and random forest experiment results

	MLP (RMSE, [°C])	random forest (RMSE [°C])
Sept 16, 2013	0.965	3.974
May 14, 2014	1.407	4.842
May 30, 2014	2.201	5.247
Oct 5, 2014	2.956	11.532
May 19, 2016	2.405	6.255

Fig. 4 is the scatter plot of the best result (Sept. 16th) and the worst (Oct. 5th). The random forest method predicts the trend of temperature well, but its dispersion of prediction and the MSE are shown to be large. Although the MLP method did not do well predicting at high temperature, the dispersion of prediction and the MSE are shown to be better.



(a) Sep 16, 2013 (MLP)

(b) Sep 16, 2013 (RF)

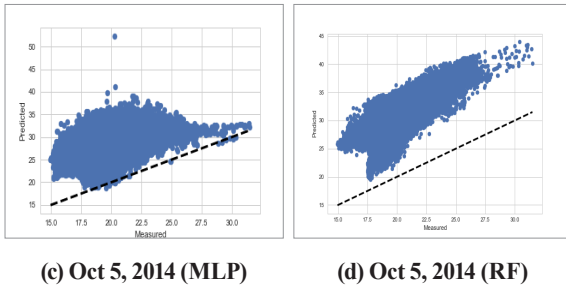


Fig. 4. Scatter plots for measured and predicted LST using MLP and random forest

3. Results and Discussion

MLP method showed less error than the random forest method. In general, MLP performs better than random forest because the relationship of independent variables are better represented through hidden layers. The RMSE of the MLP is about 1 to 3°C, while the random forest is about 4 to 11°C. Random forest predicted the trend well but showed wide variation. Both random forest and MLP predicted lower temperatures for data with higher temperatures. As shown in Figs. 4(a), (b) and (d), prediction values in the range of 30 to 40°C are more scattered than in the lower the temperature range. This can be explained by the fact that the average temperature for the training dataset were 27.49°C. This results in the model to be more accurate in the 25 to 30°C temperature range. Varied training data, encompassing all months of the year, should produce a more robust model.

4. Conclusions

This paper applied MLP to downscaling to improve the spatial resolution of 1 kilometer to 30 meters spatial resolution and temporal resolution from 16 days or more to 1 day resolution, depending of the availability of cloudless MODIS imagery. The presented MLP structure using the daily, seasonal and fixed feature data design, resulted in downscaling average error of 1-2°C. The data was divided into three categories in the design process, making it easier to add data later. The MLP method with the proposed five feature layers, showed better results than random forest method, and the predicted images were superior in visual context. The

mean RMSE of the validation was 1.92 °C and with more varied training data, better results can be anticipated. It was shown in the study, that downscaling with MLP method is feasible for temperature monitoring, urban heat island study, and abnormal temperature detection analysis of urban dense areas. The proposed downscaling method which can predict temporal resolution up to maximum 1 day will enable time series analysis for agriculture, public health, and urban planning applications.

Acknowledgment

This work was supported by the Korea Research Foundation (2015R1D1A1A01056884).

References

- Bhang, K. and Lee, J. (2017), Consideration of NDVI and surface temperature calculation from satellite imagery in urban areas: a case study for Gumi, Korea, *Journal of the Korean Society of Surveying, Geodesy, Photogrammetry and Cartography*, Vol. 35, No. 1, pp. 23-30.
- Bonafoni, S. (2016), Downscaling of Landsat and MODIS land surface temperature over the heterogeneous urban area of Milan, *IEEE Journal of Selected Topics in Applied Earth Observations and Remote Sensing*, Vol. 9, No. 5, pp. 2019-2027.
- Bonafoni, S. and Tosi, G. (2017), Downscaling of land surface temperature using airborne high-resolution data: a case study on Aprilia, Italy, *IEEE Geoscience and Remote Sensing Letters*, Vol. 14, No. 1, pp. 107-111.
- Chollet, F. (2017), *Deep Learning with Python*, Manning, New York, N.Y.
- Hutengs, C. and Vohland, M. (2016), Downscaling land surface temperatures at regional scales with random forest regression, *Remote Sensing of Environment*, Vol. 178, pp. 127-141.
- Jee, J., Lee, G., and Choi, Y. (2014), Analysis of land surface temperature from MODIS and Landsat satellites using by AWS temperature in capital area, *Korean Remote Sensing Society*, Vol. 30, No. 2, pp. 315-329.
- Keramitsoglou, I., Kiranoudis, C.T., and Weng, Q. (2013),

- Downscaling geostationary land surface temperature imagery for urban analysis, *IEEE Geoscience and Remote Sensing Letters*, Vol. 10, No. 5, pp. 1253-1257.
- Kim, N. (2016), Machine learning approaches to corn yield estimation using satellite images and climate data: a case of Iowa state, *Journal of the Korean Society of Surveying, Geodesy, Photogrammetry and Cartography*, Vol. 34, No. 4, pp. 383-390.
- Kolios, S., Georgoulas, G., and Stylios, C. (2013), Achieving downscaling of Meteosat thermal infrared imagery using artificial neural networks, *International Journal of Remote Sensing*, Vol. 34, No. 21, pp. 7706-7722.
- Park, M. (2001), A study on the urban heat island phenomenon using LANDSAT TM thermal infrared data, Vol. 21, No. 6D, pp. 861-874.
- Stathopoulou, M. and Cartalis, C. (2009), Downscaling AVHRR land surface temperatures for improved surface urban heat island intensity estimation, *Remote Sensing of Environment*, Vol. 113, No. 12, pp. 2592-2605.
- Trevor H., Robert T., and Jerome F. (2008), *The Elements of Statistical Learning*, Springer, New York, N.Y.
- Trzaska, S. and Schnarr, E. (2014), A review of downscaling methods for climate change projections, *United States Agency for International Development by Tetra Tech ARD*, pp. 1-42.
- Wilby, R.L. and Wigley, T.M.L. (1997), Downscaling general circulation model output: a review of methods and limitations, *Progress in Physical Geography*, Vol. 21, No. 4, pp. 530-548.
- Yang, G., Pu, R., Huang, W., Wang, J., and Zhao, C. (2010), A novel method to estimate subpixel temperature by fusing solar-reflective and thermal-infrared remote-sensing data with an artificial neural network, *IEEE Transactions on Geoscience and Remote Sensing*, Vol. 48, No. 4, pp. 2170-2178.
- Zakšek, K. and Oštir, K. (2012), Downscaling land surface temperature for urban heat island diurnal cycle analysis, *Remote Sensing of Environment*, Vol. 117, pp. 114-124.